Comparison of the optical properties of dissolved organic matter in two river-influenced coastal regions of the Canadian Arctic

Leira Retamal [a,*], Warwick F. Vincent [a], Christine Martineau [b], Christopher L. Osburn [c]

[a] *Département de Biologie & Centre d'Études Nordiques, Université Laval, Cité Universitaire,*
Pavillon Alexandre Vachon, Québec, Québec G1K 7P4, Canada
[b] *Département de biologie & Québec-Océan, Université Laval, Cité Universitaire, Pavillon Alexandre Vachon, Québec,*
Québec G1K 7P4, Canada
[c] *Marine Biogeochemistry Section, US Naval Research Laboratory, Code 6114, Washington, DC 20375, USA*

Abstract

The optical characteristics of coloured dissolved organic matter (CDOM) were analyzed in the Great Whale River and adjacent Hudson Bay ($55°$ N, $77°$ W) in the eastern Canadian Low Arctic, and in the Mackenzie River and adjacent Beaufort Sea in the western Canadian High Arctic ($70°$ N, $133°$ W). Sampling was during ice-free open water conditions. Both rivers contained high concentrations of dissolved organic carbon (3 and 6 mg DOC l^{-1} in the Great Whale River and Mackenzie River, respectively) and CDOM (a_{320} of 11 and 14 m^{-1}), resulting in a substantial load of organic matter to their coastal seas. There were pronounced differences in the CDOM characteristics of the two rivers, notably in their synchronous fluorescence scans (SFS). The latter showed that the Mackenzie River was depleted in humic materials, implying a more mature catchment relative to the younger, more recently glaciated Great Whale River system. SFS spectra had a similar shape across the freshwater–saltwater transition zone of the Great Whale plume, and DOC was linearly related to salinity implying conservative mixing and no loss by flocculation or biological processes across the salt front. In contrast, there were major differences in SFS spectral shape from the Mackenzie River to the freshwater-influenced coastal ocean, with a marked decrease in the relative importance of fulvic and humic acid materials. The SFS spectra for the coastal Beaufort Sea in September–October strongly resembled those recorded for the Mackenzie River during the high discharge, CDOM-rich, snowmelt period in June, but with some loss of autochthonous materials. These results are consistent with differences in freshwater residence time between the Mackenzie River and Great Whale River coastal ocean systems. Models of arctic continental shelf responses to present and future climate regimes will need to consider these striking regional differences in the organic matter content, biogeochemistry and optics between waters from different catchments and different inshore hydrodynamic regimes.
© 2006 Elsevier Ltd. All rights reserved.

Keywords: Arctic; coloured dissolved organic matter; climate change; DOC; optics; synchronous fluorescence

1. Introduction

Dissolved organic matter (DOM) plays a major role in the ocean as carbon and energy sources for the microbial food web, and for consumers at higher trophic levels that feed on microbes or on DOM directly. The coloured fraction of this dissolved organic matter is a complex pool of autochthonous materials, derived from *in situ* photosynthetic activity and processed microbially, and allochthonous materials, that are rich in humic substances and largely derived from terrestrial environments (Blough and Del Vecchio, 2002). This coloured dissolved organic matter (CDOM) is photochemically active and also influences the spectral underwater regime that in turn

affects primary production (Pienitz and Vincent, 2000; Lehmann et al., 2004). The composition and reactivity of CDOM in aquatic ecosystems are still poorly understood, however, various optical techniques, including spectrofluorescence, are providing new insights from diverse environments (McKnight et al., 2001; Peuravuori et al., 2002).

The sources and dynamics of DOM are of special interest in the coastal Arctic Ocean. These environments receive inputs of freshwater from large rivers that drain arctic tundra and peatlands as well as subarctic boreal forest. It has been estimated that more than 25% of the world's soil carbon lies in these catchments, and there is concern about how ongoing climate change may mobilise these stocks and transport them to arctic seas (Waelbroeck and Monfray, 1997; Gulledge and Schimel, 2000; Guo et al., 2003). The carbon derived from arctic rivers appears to be a major source of terrigenous DOM to the deep ocean (Opsahl et al., 1999; Dittmar, 2004), and changes in the magnitude and composition of this material therefore have broader oceanographic implications. At present, arctic rivers deliver $3300 \text{ km}^3 \text{ y}^{-1}$ of water to the Arctic Ocean (about 11% of the total freshwater input to the world ocean; Rachold et al., 2004) and 8.5 t of dissolved organic carbon $\text{km}^{-2} \text{ y}^{-1}$ (Telang et al., 1991; about 10% of the total DOM export by rivers to the world ocean; Opsahl et al., 1999). Global circulation models predict that the arctic basin will experience greater and more rapid warming than elsewhere over the course of this century, and there is increasing evidence that global climate change has already begun to have significant impacts on permafrost degradation and terrestrial vegetation dynamics at high northern latitudes (ACIA, 2004).

The objectives of the present study were to determine the CDOM properties of two northern rivers that discharge to arctic seas (Great Whale River and Mackenzie River, Fig. 1), and to evaluate how these properties change over the arctic continental shelf. Great Whale River is one of the main inflows to Hudson Bay. It lies in the forest tundra region of the eastern Canadian low Arctic and drains large areas of boreal forest in the southern parts of it catchments. The Mackenzie River is more representative of the large rivers that discharge into the Arctic Ocean. It lies in the western Canadian Arctic, 2500 km to the west of Great Whale River, and drains tundra and boreal forest, ultimately discharging its sediment and organic-rich waters into the Mackenzie shelf region of the Beaufort Sea.

We applied UV−visible and synchronous fluorescence (SFS) spectroscopic techniques to characterize these waters. Stable isotope signatures ($\delta^{13}C$ and $\delta^{15}N$) of the seston were also measured as a complementary guide to the offshore gradients in terrigenous *vs.* autochthonous carbon sources. Specially we addressed the following questions: (1) are the properties of DOM uniform among arctic inflows, as indicated
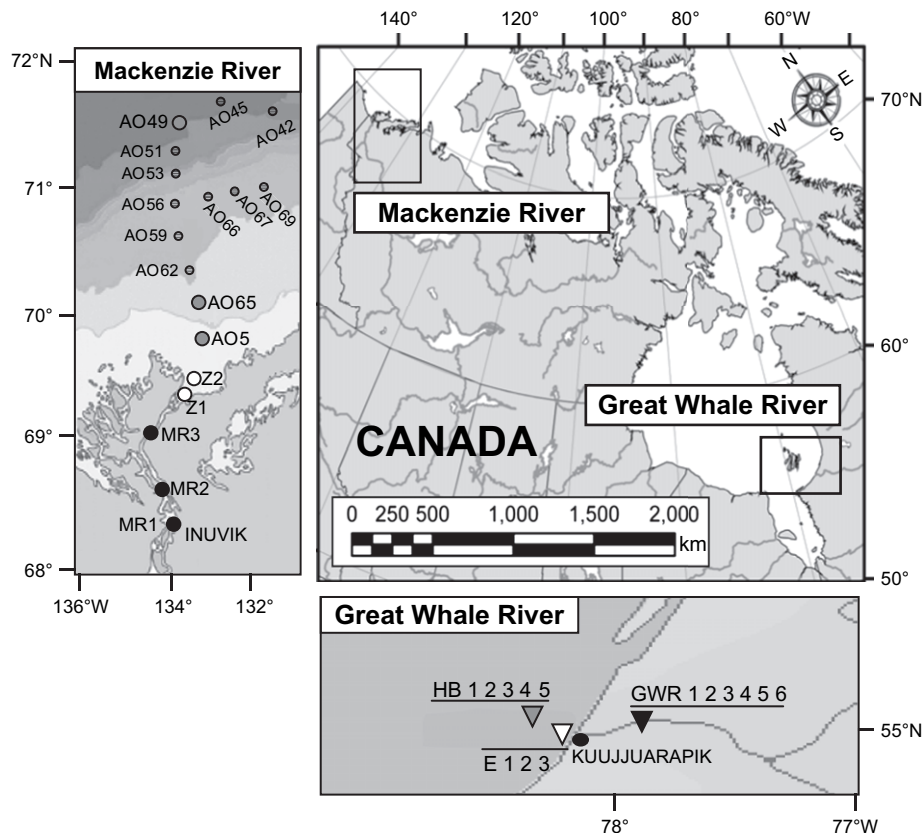

Fig. 1. The two sampling locations in northern Canada: Mackenzie River (MR, black circles); Estuarine stations (Z, white circles); and offshore Arctic Ocean stations (AO, grey circles). Additional CASES 2002 stations (partially filled circles) that were also sampled for surface absorption: Great Whale River (GWR, black triangles); Estuarine stations (E, white triangles); and Hudson Bay stations (HB, grey triangles).

by these two systems that are well-separated geographically; and (2) do DOM properties change across the estuarine transition from freshwater to marine associated with the changes in salinity. These questions are of broad interest given the current increase in water and organic matter export from rivers to the Arctic Ocean, and the likely acceleration of this trend in the future (Peterson et al., 2006; Waelbroeck and Monfray, 1997).

2. Materials and methods

2.1. Study sites

Great Whale River (GWR) is 416 km long and flows through boreal forest and forest tundra ecozones in subarctic Québec, Canada, before discharging into Hudson Bay at Kuujjuarapik (55°16'22'' N, 77°46'02'' W; Fig. 1). The 0.42×10^6 km^2 drainage area is characterized by discontinuous permafrost and its vegetation is mostly composed of black spruce and small shrubs (Hudon et al., 1996). The summer river discharge is 400–800 m^3 s^{-1}, with an annual mean of 666 m^3 s^{-1} (Goldstein and Jacobsen, 1988; Hudon et al., 1996). This system is estimated to transport 0.09×10^6 t y^{-1} of dissolved organic carbon (DOC) into Hudson Bay (Hudon et al., 1996).

The Mackenzie River (MR) is the longest river in Canada (1600 km) and discharges into the Beaufort Sea at Tuktoyaktuk (70°8'45'' N, 133°30'41'' W; Fig. 1). For 2002 the summer discharge at a downstream site (Arctic Red River station 10LC014) varied from 9640 to 21,100 with values around 13,000 m^3 s^{-1} during the fall period of sampling. The drainage area is 1.707×10^6 km^2 and begins at Great Slave Lake, itself fed by many tributaries and rivers from the western subarctic and arctic regions of Northwest Territories. Large expanses over the northern parts of the Mackenzie basin are underlain by permafrost, even in the sediments of the marine delta (Millot et al., 2003). The vegetation cover is mainly composed of boreal forest in the northern and western mountainous parts of the catchment. The northeastern part of the basin contains tundra, while the lowlands of the central basin are occupied by deciduous forest, riparian spruce and abundant thermokarst lakes and peatland (Millot et al., 2003; Spears and Lesack, 2006 and references therein). The Mackenzie River system is estimated to deliver an annual load of 2.65×10^6 t of DOC into the Beaufort Sea (Telang et al., 1991). It also delivers 2.1×10^6 t of particulate organic carbon (POC), the largest riverine POC loading of all the arctic inflows (Droppo et al., 1998; Rachold et al., 2004).

Sampling was undertaken during open water conditions in July–August (GWR) and September–October (MR) of 2002. Surface water samples were obtained at freshwater sites (GWR and MR stations) in each river, estuarine stations (E and Z series) and marine sites over the continental shelf in Hudson Bay (HB) and the western Arctic Ocean (AO) along transects perpendicular to the coast. Additional samples from the Mackenzie River (MR3) were taken during the period of high discharge on 17 June 2004 (flows at that time were 60% of the peak snowmelt discharge of about 30,000 m^3 s^{-1}

that occurred in late May), and from two major tributaries of the Mackenzie River, the Arctic Red River (ARR) and Peel River (Peel), in August 2004. Both of these tributaries flow from mountain catchments to the tundra and join the Mackenzie River approximately 25 km before its discharge into the sea.

2.2. Suspended particulate material (SPM)

SPM samples were filtered onto pre-combusted and pre-weighed, 47 mm diameter GF/F filters (nominal pore size 0.7 μm) and then stored frozen until laboratory analysis. Filters were oven-dried at 60 °C overnight, cooled to room temperature in a desiccator and re-weighed.

2.3. DOM sampling

Samples were filtered through sterile 0.22-μm Nuclepore membrane filters and the filtrate was then stored in acid-washed, sample-washed amber bottles in the dark at 4 °C until further analysis. Samples were subsequently analyzed within 2 months of collection for CDOM absorption, synchronous fluorescence properties (SFS) and for dissolved organic carbon concentrations. To test for any effects of storage we repeated SFS measurements on 0.22-μm filtered Great Whale River samples after 5 months of storage at 4 °C. This showed no change in spectral form, with peak fluorescence at 300 nm of 1.25 QSU (quinine sulfate units) in the initial scan, and 1.20 QSU at the end of the 5 months (3% change).

2.3.1. CDOM absorption measurements

CDOM absorption was measured in acid-cleaned 10-cm quartz cells using a Hewlett–Packard 8452A diode array spectrophotometer (GWR samples) and a Varian Cary Bio 300 scanning spectrophotometer (MR samples). Samples were scanned at 2 nm intervals between 250 and 820 nm (HP 8452A) and at 1 nm intervals between 200 and 850 nm (Cary Bio 300), against MilliQ pure water. The spectrum was corrected for the absorption offset using the mean value for wavelengths greater than 800 nm.

The absorption coefficients were calculated as:

$$a(\lambda) = 2.303 \times A(\lambda)/L$$

where $A(\lambda)$ is the optical density for wavelength λ and L is the cell path length in metre. The CDOM properties were modeled using a non-linear regression from 300 and 650 nm for the relationship:

$$a(\lambda) = a_{320} \times e^{S(320-\lambda)}$$

where a_{320} is the absorption coefficient at 320 nm and S is the slope of the regression. The regression coefficients (r^2) for all curves were greater than 0.997, so the need to add a constant to the regression model for a better fit was not considered

necessary for these high CDOM containing waters (Stedmon et al., 2000).

2.3.2. Synchronous fluorescence spectroscopy (SFS)

This technique provides a guide to the chemical structure, complexity, degree of humification as well as the molecular weight of CDOM (Kalbitz and Geyer, 2001; Peuravuori et al., 2002; Kowalczuk et al., 2003). Complex molecules of low molecular weight (less than 5000 Da) fluoresce when excited at shorter wavelengths (280−323 nm) and likely represent autochthonous organic matter (including protein-like compounds) coming from *in situ* biological processes such as primary production, detritus production and 'sloppy feeding' by zooplankton. Molecules of medium molecular weight (approximately 15,000 Da and smaller than 30,000 Da) are more complex compounds, typically fulvic acids coming from autochthonous but mostly allochthonous processes, and their maximum emission is located between 324 and 432 nm. Humic acids fall in the high molecular weight group and fluoresce maximally at higher wavelengths (433−593 nm) (Chen et al., 2003). In addition to the overall scans we used the ratio of integrated areas under the spectrum of these three wavebands as an index of CDOM composition and state of transformation (Kalbitz and Geyer, 2001): $L\lambda/H\lambda$ as the ratio of fluorescence integrated over the waveband 280−323 nm to that over the waveband 433−595 nm, and $M\lambda/H\lambda$ as the ratio of integrated fluorescence 324−432 nm to integrated fluorescence 433−595 nm.

Samples were scanned over the excitation wavelength range 200−600 nm in acid-cleaned 1-cm quartz cells with a Shimadzu FR5000 spectrofluorometer (for GWR samples) and with a Cary Eclipse 3000 (for MR samples). For both instruments, the scans were made in synchronous mode with a slit width of 5 nm on both sides and a constant difference between the excitation and emission wavelengths of 14 nm (Belzile et al., 2001). The spectra were corrected for the baseline, and for inner filter effect using the absorption data for each sample, as in Mobed et al. (1996). Both instruments were checked for wavelength accuracy using the Raman peak for water. This confirmed the accuracy of the Cary and showed a 3-nm red shift for the Shimadzu. A correction for this minor wavelength offset was applied to the Shimadzu scans. For quantitative comparisons, the fluorescence output from both fluorometers was converted to quinine sulfate units (QSU) using a standard of quinine sulfate dihydrate (Sigma−Aldrich no. 22640) dissolved in 0.02 N sulfuric acid (Velapoldi and Mielenz, 1980). The two instruments were cross calibrated with the same quinine sulfate solution and the fluorescence output was expressed on the same QSU scale for both instruments. The quinine sulfate solution had the same spectral shape in both instruments, with the 3 nm offset for the Shimadzu as detected in the Raman tests. The scans were subsequently smoothed with a second order polynomial using a single wavelength-step forward (SigmaPlot 8.0). To enhance spectral differences and hidden peaks for a more detailed analysis of spectra, the second derivative of the SFS scans was calculated with the Savitzky−Golay algorithm in the program PeakFit version 4.0. Derivative analysis has been previously used to analyze fluorescence in organic mixtures (Patra and Mishra, 2002) and in the optical analysis of other complex multicomponent systems, for example to identify pigment peaks in natural phytoplankton absorption spectra (Millie et al., 1997).

2.3.3. Dissolved organic carbon

DOC concentrations were obtained by high temperature oxidation using a Shimadzu TOC Analyser 5000A with detection limits of 0.05 mg l^{-1} over the range 1−10 mg l^{-1} using $KHC_8H_4O_4$ as the carbon standard. Before analysis, samples were acidified with 0.01 N HCl to a final pH of 2.0 and then bubbled with CO_2-free nitrogen for a prolonged period (7 min) to ensure the removal of all DIC, as recommended for carbonate-rich waters (Sharp et al., 1993).

2.4. Isotopic analysis of POM

Two to five litres of surface water were collected at each site along the freshwater−saltwater transect on the GWR and MR. Water was kept cold until filtration of the suspended particulate organic matter (POM) onto pre-combusted (500 °C, 1 h) Whatman GF/F filters. These were stored frozen at −20 °C until subsequent analysis. Samples were acidified with fuming 36% HCl (Kendall et al., 2001; Yamamuro and Kayanne, 1995) and oven-dried at 60 °C overnight. Isotopic analysis was carried out at the Commission Géologique du Canada using a CF-IRMS (Fisons Instruments, model VG Prism Isotech) coupled with an Elemental Analyser (NA 2500 series). Stable isotope ratios were expressed in per mil notation (‰) according to the equation:

$$\delta X = \left[\left(R_{sample} / R_{standard} \right) - 1 \right] \times 1000$$

where X is ^{13}C or ^{15}N and R is the corresponding ratio $^{13}C/^{12}C$ or $^{15}N/^{14}N$ relative to PeeDee Belemnite and atmospheric nitrogen standard values. The internal standards were vanillin (Sigma−Aldrich) and USGS-25 for carbon and urea (Sigma−Aldrich), IAEA-N1 and IAEA-N2.

3. Results

3.1. CDOM absorption parameters

The a_{320} measurements showed high CDOM concentrations in both rivers, with highest values in the Mackenzie River, particularly during the high discharge period (MR3, Fig. 1). In the Great Whale River system, a_{320} dropped by 27% at the estuarine station (E) and to 55% of riverine values at the offshore Hudson Bay station (HB), and was an inverse function of salinity ($r = -0.984$; $p < 0.0001$) (Table 1, Fig. 2c). The means for each of the sites were significantly different from each other (non-parametric Tukey tests: GWR *vs.* HB, $q = 11.98$; $p = 0.001$; GWR *vs.* E, $q = 5.11$; $p = 0.011$; HB *vs.* E, $q = 4.98$; $p = 0.012$).

Table 1
Chemical and optical data from the Great Whale River and Mackenzie River systems. DOC, dissolved organic carbon concentration; a_{320}, the absorption coefficient at 320 nm; a_{320}^*, the absorption coefficient normalized by DOC concentration; S, the spectral slope for light absorption by CDOM; and SPM, the total suspended particulate matter. Values in parentheses are SE. Note that MR3 is for the high discharge period in 2004

Station	Date	Salinity	DOC (mg C l^{-1})	a_{320} (m^{-1})	a_{320}^* (m^2 g^{-1})	S (nm^{-1})	SPM (mg l^{-1})
Great Whale River and Hudson Bay River							
GWR1-0m	23/07/2002	0.02	2.8	11.61	4.15	0.0156	6.98
GWR2-0m	26/07/2002	0.04	2.7	11.32	4.20	0.0158	7.23
GWR3-0m	03/08/2002	0.02	2.7	10.92	4.04	0.0158	8.14
GWR4-0m	05/08/2002	0.04	2.9	10.94	3.77	0.0168	8.40
GWR5-0m	07/08/2002	0.03	3.8	11.86	3.12	0.0159	12.18
GWR6-0m	08/08/2002	0.04	3.0	11.90	3.97	0.0161	10.30
Mean river			2.98 (0.17)	11.42 (0.18)	3.88 (0.16)	0.0160 (0.0002)	8.87 (0.82)
Estuary							
E1-0m	24/07/2002	19.91	2.70	5.53	2.05	0.0157	12.99
E2-0m	30/07/2002	0.03	2.70	10.90	4.04	0.0158	9.48
E3-0m	04/08/2002	12.97	2.70	8.49	3.14	0.0157	6.42
Mean estuary			2.70	8.307 (1.55)	3.08 (0.58)	0.0157	9.63 (1.9)
Offshore							
HB1-0m	22/07/2002	24.65	2.22	4.73	2.13	0.0167	10.02
HB2-0m	25/07/2002	24.65	2.94	4.91	1.67	0.0165	15.37
HB3-0m	28/07/2002	23.17	2.56	5.33	2.08	0.0170	11.42
HB4-0m	01/08/2002	24.48	2.36	4.95	2.10	0.0174	14.30
HB5-0m	08/08/2002	24.61	2.26	5.93	2.62	0.0185	15.60
Mean offshore			2.47 (0.13)	5.17 (0.21)	2.12 (0.15)	0.0172 (0.0003)	13.32 (1.12)
Mackenzie River and Beaufort Sea River							
MR1-0m	08/10/2002	0.07	5.70	14.37	2.52	0.0179	42.51
MR2-0m	08/10/2002	0.07	4.90	12.18	2.49	0.0192	27.84
Mean river (October)			5.30 (0.40)	13.28 (1.10)	2.51 (0.02)	0.0185 (0.0006)	35.18 (7.34)
MR3-0m (June)	17/06/2004	0.07	4.80	16.87	3.53	0.0172	99.02
Estuary							
Z1-0m	02/10/2002	24.46	1.60	2.02	1.26	0.0176	60.38
Z2-0m	03/10/2002	25.44	2.47	1.91	0.77	0.0182	17.26
Mean estuary			2.04 (0.44)	1.97 (0.08)	1.02 (0.25)	0.0179 (0.0003)	38.82 (21.5)
Offshore							
AO5-0m	03/10/2002	30.09	1.15	0.87	0.76	0.0195	12.65
AO65-0m	02/10/2002	26.88	0.88	0.68	0.77	0.0254	1.75
AO49-0m	28/09/2002	26.37	1.14	0.60	0.53	0.0217	0.96
Mean offshore			1.06 (0.09)	0.72 (0.08)	0.69 (0.08)	0.0222 (0.003)	5.12 (3.77)

The Mackenzie River showed a more complex pattern with an initial 6.5-fold decrease at the Z stations, then variable changes to minimum values for the transect towards the edge of the arctic pack ice at station AO49 (0.60 m^{-1}). There was a patch of increased a_{320} at stations AO66 (2.42 m^{-1}) and AO56 (3.33 m^{-1}) (AO66 and AO56 only absorption properties were available). This pattern is consistent with the mixing of the MR plume with seawater 90–170 km offshore. This offshore plume was isolated from the coast by high salinity water at stations AO5 and AO65 associated with wind-induced, inshore upwelling (details in Garneau et al., 2006). The Mackenzie River system also showed a linear decrease in a_{320} with increasing salinity ($r = -0.934$; $p = 0.002$; Fig. 2c), however, the absence of samples at intermediate salinities means that this relationship should be interpreted with caution.

The absorption spectra for the Great Whale River system remained relatively constant between sampling times for the river and HB stations, and varied between the two extremes in the estuarine transition zone, depending on the extent of

mixing (Fig. 2a). Spectral slope increased offshore as a non-linear function of salinity, with a sharp rise in S-values at salinities above 20 to a maximum of 0.0185 nm^{-1} (Fig. 2d). The river and estuarine surface samples (within the plume) did not differ significantly in spectral slopes ($n = 3$; $F = 9.20$; $p = 0.76$), but the mean offshore (HB) S-value was significantly higher relative to the river and estuarine stations ($n = 3$; $p = 0.010$ and 0.009, respectively).

The Mackenzie River absorption spectra also showed a pronounced offshore gradient (Fig. 2b, c). There was an overall trend of increasing spectral slope with distance offshore, with a value of 0.0217 nm^{-1} at the edge of the arctic pack ice (Table 1). The highest value, however, was in the oceanic water mass at Station AO65 (0.0254 nm^{-1}). The river as well as offshore sites were significantly above those for the Great Whale River system (GWR $vs.$ MR, $t = 5.8$, $p = 0.001$; HB $vs.$ AO, $t = 4.05$; $p = 0.007$). The Mackenzie S-values were a non-linear function of salinity, with an abrupt rise above 20 (Fig. 2d), similar to that observed in the Great Whale River
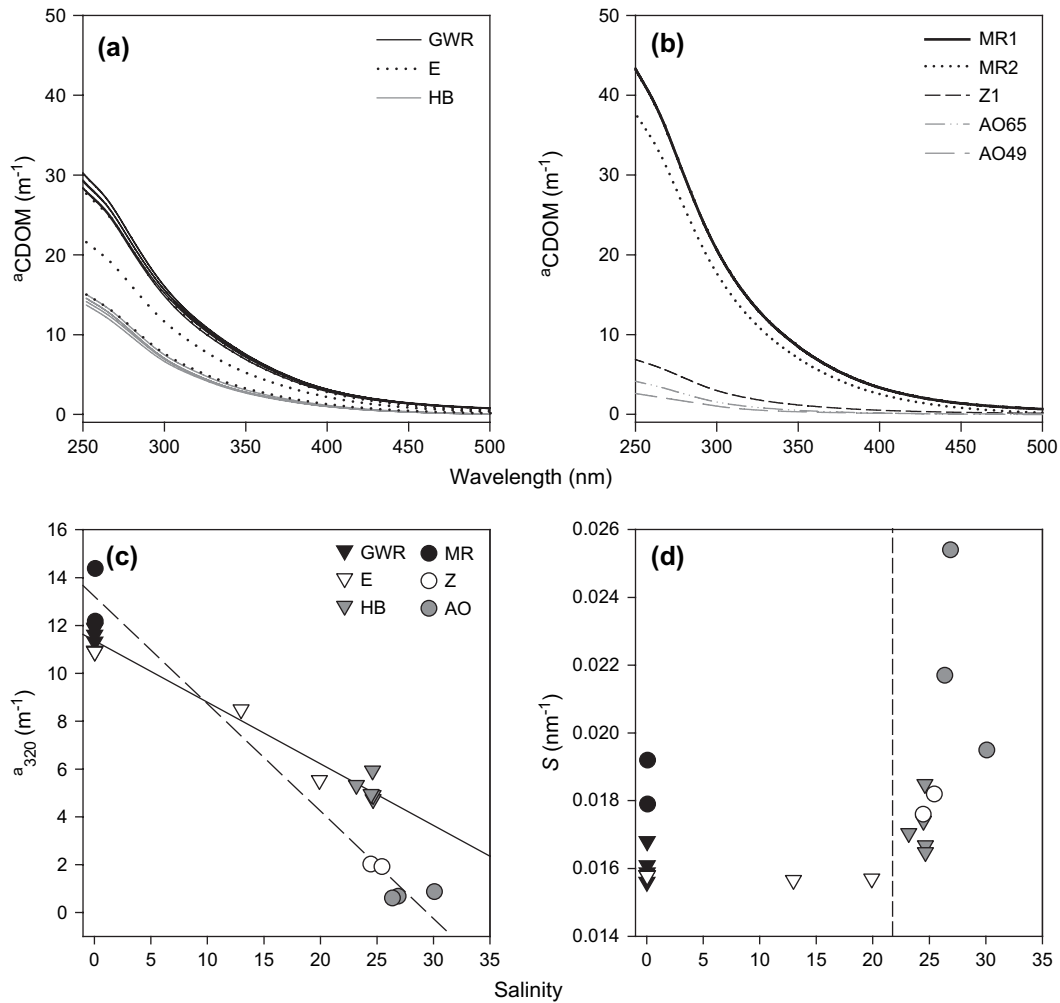
Fig. 2. Comparison of CDOM absorption properties among sites. (a) CDOM absorption in the Great Whale River system. Surface water samples at river stations (GWR), estuarine stations (E) and in offshore Hudson Bay (HB). (b) CDOM absorption in the Mackenzie River system. Surface water samples at river stations (MR1 and MR2), estuarine station (Z1) and in offshore stations AO65 and AO49. (c) CDOM absorption at 320 nm *vs.* salinity for the two rivers. Surface water samples in the Great Whale River system (abbreviations as above) and Mackenzie River system (MR, river stations; Z, estuarine stations Z1 and Z2; AO, offshore stations AO5, AO65 and AO49). Lines are for least squares linear regressions. (d) Exponential slope coefficients (S-values) for the absorption *vs.* wavelength curves as a function of salinity in the Great Whale River system (triangles) and Mackenzie River system (circles). Symbols are as that of (c).

data set, however, there were no statistically significant differences in spectral slope among groups of stations (MR *vs.* Z, $q = 0.426$, $p = 0.952$; Z *vs.* AO, $q = 3.398$, $p = 0.150$; MR *vs.* AO, $q = 2.931$, $p = 0.211$).

The DOC-specific values for CDOM absorption (a^*_{320}) were 50% higher in the Great Whale River than in the Mackenzie River (autumn) ($t = 4.60$; $p = 0.004$). Highest a^*_{320} values in the Mackenzie River were recorded during the high discharge period in June, within the range observed in GWR. In the 2002 transect, there was a significant drop in a^*_{320} between the Mackenzie River and the coastal and offshore stations (MR *vs.* Z, $q = 10.6$; $p = 0.004$; MR *vs.* AO, $q = 14.2$, $p = 0.001$), but there was no statistical difference between the coastal and the offshore samples ($q = 2.56$, $p = 0.28$). In the GWR system, there was similarly a significant drop in a^*_{320} between the GWR and HB ($q = 7.55$, $p < 0.001$) but no significant difference between GWR and E ($q = 2.94$, $p = 0.14$) nor between the inshore and offshore stations (E *vs.* HB, $q = 3.41$, $p = 0.081$).

3.2. Synchronous fluorescence spectra

The spectral shape of the SFS for the Great Whale River system was similar at all stations and sampling times, but there was a pronounced decrease in absolute fluorescence intensities offshore (Fig. 3a). A peak was present near 300 nm (corresponding to the emission wavelength of protein-like substances) in all samples and showed little change across the salinity gradient. A second peak was apparent within the fulvic acid range near 400 nm and a third peak occurred in the terrestrial humic acid range around 500 nm. This latter peak was more variable than the other two, and was much lower in the estuarine and saltwater relative to freshwater samples. The second derivative curves were similar at all stations, implying a relative constancy in the CDOM pool (Fig. 3a), and suggesting that minor components of the signature were not substantially enriched or modified during transport across the estuary.
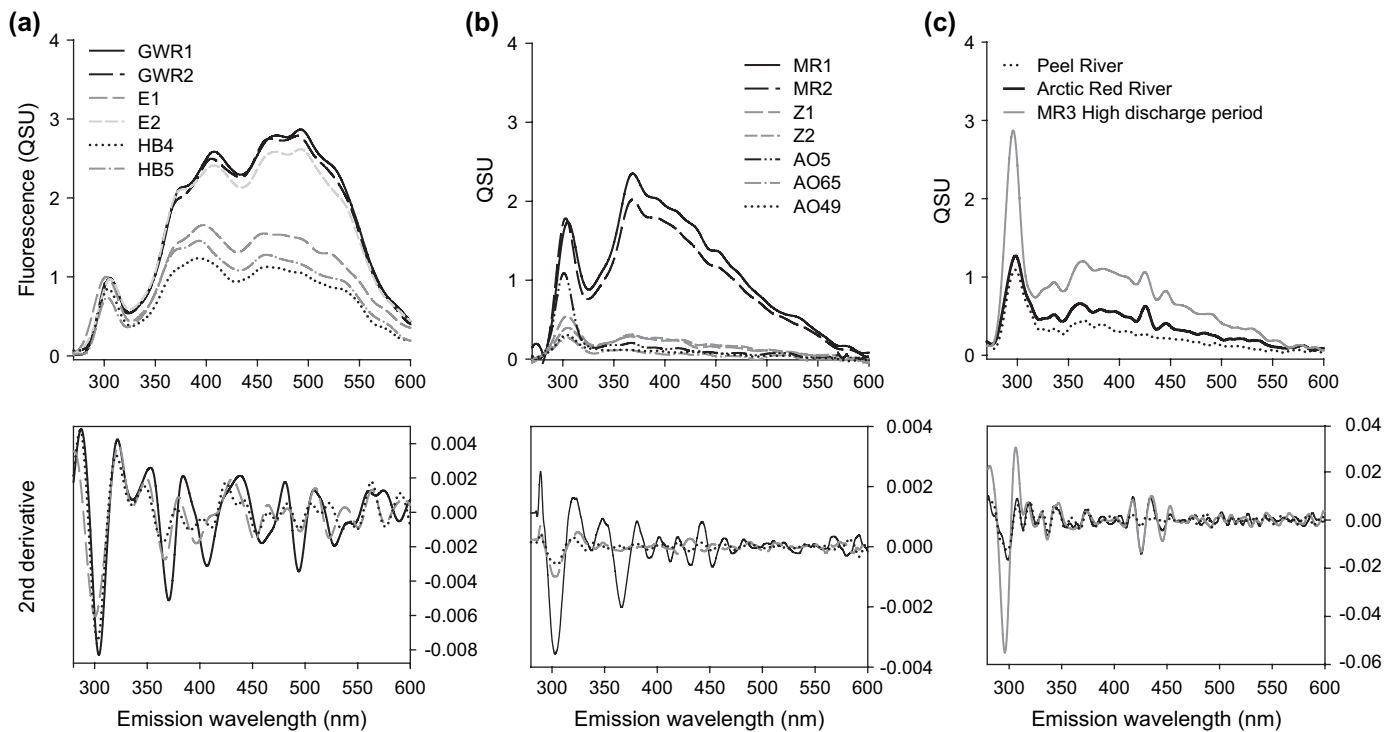
Fig. 3. Comparison of synchronous fluorescence spectra at each site. (a) Great Whale River system, 2002. (b) Mackenzie River system, 2002. (c) Mackenzie River during the high discharge period at site MR3, June 2004; two tributaries of the Mackenzie sampled in August 2004, Peel River and Arctic Red River. Lower panels: second derivative curves for SFS spectra at each site.

The spectrofluorescence signatures of the Mackenzie River system differed greatly from those of the Great Whale system, with a low contribution in the $H\lambda$ fluorescence range and a pronounced $L\lambda$ peak at 300 nm at all stations (Fig. 3b). The $L\lambda$ peak was particularly striking in the Mackenzie River sample obtained during high discharge in June (Fig. 3c). Samples from two upstream tributaries of the Mackenzie River, sampled in late July 2004, also showed maximum fluorescence at 300 nm (Fig. 3c). The two MR stations in the 2002 transect showed high fluorescence in the waveband 323–600 nm indicative of a terrestrial influence (Fig. 3b), however, $H\lambda$ range fluorescence was reduced especially relative to the Hudson Bay series (Fig. 3a). The broad $M\lambda$ maximum found in the river was not apparent at the coastal marine stations (Fig. 3b) and the spectra for these sites were closer to the fluorescence signature from the high discharge period and from the two main tributaries (Fig. 3c). These similarities were further apparent from the second derivative analyses of MR3 and Z1.

The SFS peak ratios provide a further guide to changes offshore and between sites. $L\lambda/H\lambda$ remained consistently below 1 throughout the Great Whale transect and increased linearly with salinity (Fig. 4a; $r = 0.901$, $p < 0.0001$). The $M\lambda/H\lambda$ ratio was near 1 throughout this system with a slight linear increase across the salinity gradient (Fig. 4a; $r = 0.936$, $p < 0.0001$). Both SFS ratios were strongly and negatively correlated with a_{320} ($r = -0.944$, $p < 0.0001$ for $M\lambda/H\lambda$; $r = -0.939$, $p < 0.0001$ for $L\lambda/H\lambda$). The $M\lambda/H\lambda$ peak ratios were significantly correlated with spectral slope ($r = 0.621$, $p = 0.018$), but there was no significant relationship between the $L\lambda/H\lambda$ ratio and S (Fig. 5a).

The $L\lambda/H\lambda$ ratio in the Mackenzie River system increased markedly along the transect, from less than 2 at the freshwater sites to a maximum of 14 in the offshore. The $M\lambda/H\lambda$ ratio ranged from 2 to 6, with highest values offshore (Fig. 4b). Both peak ratios were non-linearly related to salinity (Fig. 4b) and a_{320} (Fig. 4d). The ratios increased offshore and were positively correlated with the spectral slope ($L\lambda/H\lambda$ *vs.* S-values, $r = 0.772$; $p = 0.042$; $M\lambda/H\lambda$ *vs.* S-values, $r = 0.929$; $p = 0.0025$; Fig. 5b).

3.3. Isotopic ratios of POM

The isotopic composition of the seston was used as an additional tracer of the terrigenous influence on coastal waters. In the Great Whale River system there was a gradual enrichment from freshwater to saltwater stations in both $\delta^{13}C$ and $\delta^{15}N$. POM carbon isotopic ratios increased by 3.9‰ from the river to offshore Hudson Bay stations, while the $\delta^{15}N$ values range increased by 1.4‰. In the more turbid Mackenzie River system, there was a stronger upward shift in the ratios along the salinity gradient between the river and the offshore Beaufort Sea, with an increase of $\delta^{13}C$ by 6.6‰ and an increase of $\delta^{15}N$ by 6.3‰ (Table 2). The high discharge sample from the Mackenzie River (MR3) was extremely turbid with a SPM concentration that was 2–4 times higher than in October 2002, and an order of magnitude above those recorded in the GWR (Table 1). The POM from MR3 was substantially enriched in $\delta^{13}C$ and $\delta^{15}N$ relative to the samples obtained in autumn 2002 implying major differences in C and N sources between sampling dates.

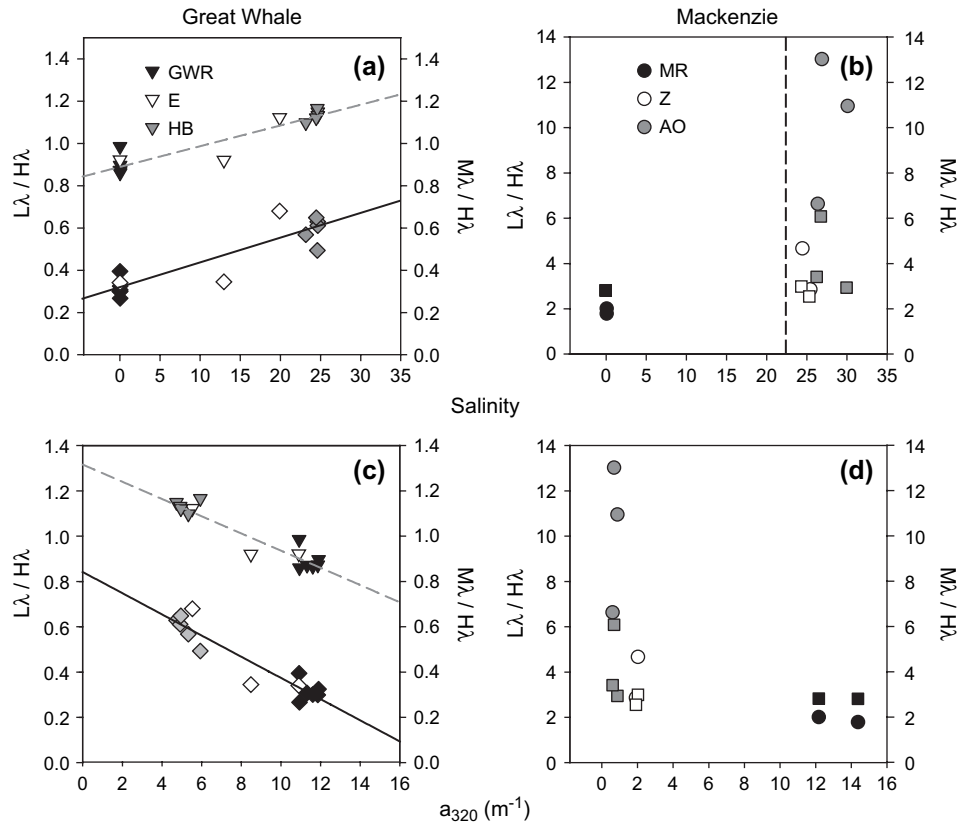Fig. 4. SFS peak ratios as a function of salinity and absorption. (a) *Lλ/Hλ* ratios (diamonds) and *Mλ/Hλ* ratios (triangles) *vs.* salinity for the Great Whale River. Curves are for linear least squares regressions (black for *Lλ* peak ratio and grey for *Mλ* peak ratio). (b) *Lλ/Hλ* ratios (circles) and *Mλ/Hλ* ratios (squares) *vs.* salinity for the Mackenzie River. Note the rise in values beyond a salinity of 22; symbols are as that of Fig. 2. (c) *Lλ/Hλ* ratios (diamonds) and *Mλ/Hλ* ratios (triangles) *vs.* CDOM absorption for the Great Whale River. (d) *Lλ/Hλ* ratios (circles) and *Mλ/Hλ* ratios (squares) *vs.* CDOM absorption for the Mackenzie River (dashed line demarcates the salinity above which there is a large variability in fluorescence ratios).

4. Discussion

As elsewhere in the Arctic Basin, the Mackenzie River and Great Whale River contained high concentrations of DOC and CDOM, and several features attest to the extensive influence of these inputs on the estuarine and coastal shelf environments that they discharge into. CDOM absorption remained high offshore, with values exceeding $2 \, \text{m}^{-1}$ more than 150 km from the coast in the Mackenzie River transect. Similarly, the SFS scans showed evidence of *Lλ* and *Mλ* signals well offshore. These observations are consistent with previous measurements in arctic coastal waters. For example the DOC-rich Lena River
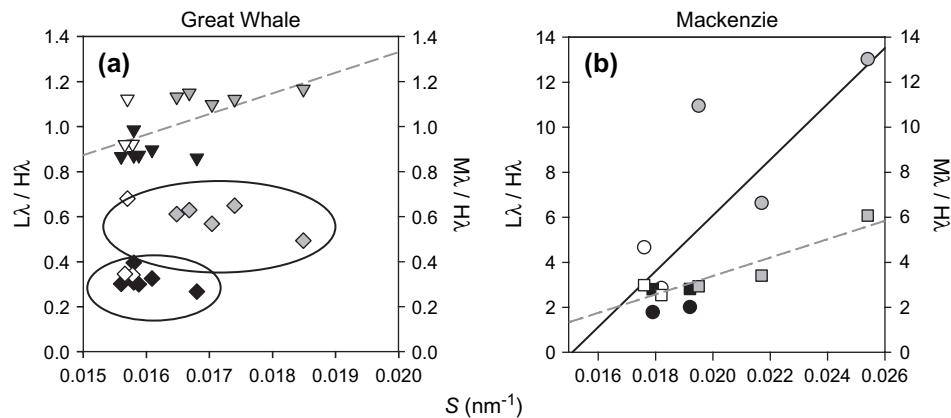

Fig. 5. SFS peak ratios as a function of spectral slope (*S*-values). (a) *Lλ/Hλ* ratios (diamonds) *vs. S* and *Mλ/Hλ* ratios (triangles) for the Great Whale River. Ellipses represent clusters of similar values of *Lλ/Hλ* ratios. (b) *Lλ/Hλ* ratios (circles) *Mλ/Hλ* ratios (squares) *vs.* spectral slope for the Mackenzie River. Curves are for linear least square regressions (dashed grey for *Mλ/Hλ* and black for *Lλ/Hλ*).

Table 2

Isotopic analysis of seston from Great Whale River (GWR) and Mackenzie River (MR) and their offshore waters. Each value for GWR is the mean of four samples (SD) obtained during summer 2002. Each MR value is from a single sample obtained during autumn 2002, with the exception of MR3 which was sampled during high discharge period, June 2004

Station	Isotopic abundance (‰)	
	$\delta^{13}C$	$\delta^{15}N$
Great Whale River and Hudson Bay		
GWR-0m	−31.68 (0.5)	1.79 (1.13)
E-0m	−30.68 (0.5)	1.90 (1.49)
HB-0m	−27.78 (1.9)	3.14 (1.92)
Mackenzie River and Arctic Ocean		
MR1-0m	−31.48	1.27
MR2-0m	−31.24	2.29
MR3-0m	−25.10	4.6
Z2-0m	−31.54	3.01
AO65-0m	−30.61	6.54
AO49-0m	−24.89	7.97

plume is known to extend up to 400 km offshore (Cauwet and Sidorov, 1996), and high CDOM absorption was recorded more than 50 km offshore over the Mackenzie Shelf by Guéguen et al. (2005).

The isotopic data in each transect also reflects the strong riverine influence on the coastal ocean, with $\delta^{13}C$ of inshore marine seston approximating that of the river and only a slight decrease offshore. Most of the river values were light (less than −30‰) relative to terrigenous plant material (e.g., −27‰ for C3 plants; Kendall et al., 2001) suggesting provenance from other sources such as freshwater phytoplankton and aquatic macrophytes. These values lie close to those previously obtained in the freshwaters of the James Bay area in northern Québec (mean $\delta^{13}C$ of −31.4‰; Montgomery et al., 2000). During the period of high discharge in the Mackenzie River (MR3), a more enriched value was recorded, and both this and the high SPM concentrations indicate a much stronger terrigenous input at this time. This is consistent with and extends the observations by Finlay et al. (2006) who measured a major increase in DOC concentrations during spring flows in the Kolyma River, Siberia, and estimated that 48% of the annual DOC flux from this river occurs during the weeks of peak snowmelt discharge. Terrigenous POM fluxes to the coastal Arctic Ocean may also be disproportionately high during this period of spring flow. The $\delta^{13}C$ value for MR3 (−25.1‰) is close to the values obtained by Goñi et al. (2005) of POM in June–July samples from the Mackenzie River. These authors also note the temporal variability in downstream POM composition and attribute this to variations in the contribution of sediment from different sources, notably from Arctic Red River and Peel River that discharge most of their sediment load in May and June.

In both transects, $\delta^{15}N$ values for POM showed a gradual rise with distance from the river mouth, consistent with the increasing influence of marine phytoplankton (Minagawa et al., 1991) and an increasing enrichment of the POM by autochthonous nitrogen. The $\delta^{13}C$ value at MR station AO49

at the edge of the pack ice (−24.9 ‰) lies close to values obtained from samples elsewhere of ice edge phytoplankton and sea ice algae (e.g. UDOM of −22.1 ‰, Opsahl et al., 1999; −23.6 ‰ for TOC, Naidu et al., 2000).

Despite these similarities, there were also fundamental differences between the two systems. The Mackenzie River had almost twofold higher DOC concentrations and was strikingly different from the Great Whale River in its spectroscopic properties, implying major qualitative differences in its CDOM content. The spectral slopes of absorption curves for the MR stations were higher than for GWR samples. This indicates the presence of older more degraded humic substances that are resistant to subsequent breakdown (Thurman, 1985; Yunker et al., 1995). The Mackenzie DOM was less coloured than in the GWR, with 30% lower DOC-specific absorption (a_{320}^*), again implying greater breakdown. This difference may, however, be seasonal because the MR3 sample during high discharge had a greater a_{320}^* value, within the GWR range. Most strikingly, the SFS spectra differed substantially between the two systems. The Mackenzie River had conspicuously weaker $H\lambda$ fluorescence than the Great Whale River indicating lower concentrations of terrestrial humic materials. These MR spectra differ from the usual riverine pattern and are more consistent with that found in organic matter from degraded peatland (Kalbitz et al., 2000) and from fen groundwater (Kalbitz and Geyer, 2001).

The differences in fluorescence spectra between the two systems could in part be a result of differences in pH (Pullin and Cabaniss, 1995; Cassasas et al., 1995). GWR is circumneutral (pH = 6.5–7) while MR is alkaline (≥7.5; Millot et al., 2003). Higher pH causes ionization of phenolic hydroxyl groups, disruption of inter- and intra-molecular hydrogen bonds, and decoiling of macromolecular structures, resulting in a lower fluorescence intensity of higher molecular weight compounds (Miano and Senesi, 1992). However, the pH difference between GWR and MR is too small to cause the magnitude of SFS differences observed. It is more likely that much of this spectral difference reflects the maturity of the respective catchments, with the more recently deglaciated GWR system releasing younger, less degraded organic material. ^{14}C-dating of samples from several arctic rivers has shown that the DOC is relatively young (Benner et al., 2004). However, ^{14}C-dating of POM in the Mackenzie River has shown that it is dominated by old (>7000 years), highly altered carbon. Goñi et al. (2005) suggest that this could be the result of inputs from fossil bitumen or kerosene in the catchment as well as highly degraded soil material that is characteristic of old permafrost soils with slow turnover rates. The MR fluorescence spectra would be consistent with DOC inputs from pre-aged, ancient soils (paleosols) that have experienced a long residence time within the Mackenzie River drainage basin.

The two systems also differed in the behaviour of CDOM across the freshwater–saltwater interface. The linear relationship between a_{320} and salinity in the Great Whale system implies conservative mixing (Stedmon and Markager, 2003). Similarly, the SFS analysis for GWR showed a close match in spectral shape between the river and bay sites, with

a decrease in concentration as might be expected for simple dilution. The $M\lambda/H\lambda$ changed with salinity, but over a narrow range, and the $L\lambda/H\lambda$ ratio similarly shifted by only a small extent. This implies a relatively minor effect of salinity, pH (which increased by 1 pH unit from the river to the sea) and other environmental changes across the transition on CDOM properties.

A similar analysis for the Mackenzie River site is limited by the lack of intermediate salinities between freshwater and fully marine and a test of conservative mixing cannot be reliably made based on a_{320}. Another study in the region over salinities 5−25 showed a strong linear relationship between a_{355} and salinity implying conservative behaviour over that range (Guéguen et al., 2005). However, greatest changes might be expected at the first encounter between freshwater and the sea, at salinities less than 5, and cannot be resolved from the absorption data in either study. The difference in pH between the river and the sea was less than 0.5 units. Further, Millot et al. (2003) demonstrate that the MR has high concentrations of ionic species. Therefore, effects of changing ionic strength and pH on CDOM properties across the MR transition zone seem unlikely.

The SFS curves for the Mackenzie River system differed greatly from those for the GWR in that they showed large differences in spectral shape between the river and offshore sites. Specifically, SFS ratios for the Mackenzie indicate a major decrease in the coastal waters of $H\lambda$ and $M\lambda$ relative to $L\lambda$ components (Fig. 4a). Such changes could imply differential loss processes operating across the salinity gradient, and deviation from conservative behaviour.

DOC flocculation is known to take place across the salt front of some estuarine transition zones and might be expected to act differentially on the larger polymers. Our analysis is limited by the absence of data from intermediate salinities, however, the comparison of freshwater and marine end members indicates that there was no greater loss of the $H\lambda$ relative to $M\lambda$ fractions in the MR system. A study on another large arctic river, the Yenisei, concluded that flocculation did not affect riverine dissolved organic matter, and DOM entered the outer shelf of the Arctic Ocean largely unaltered (Lobbes et al., 2000; Köhler et al., 2003). The MR river water is rich in particles relative to other arctic rivers, and in the present study showed four times higher concentrations of suspended particulate matter relative to GWR. These high concentrations of particles in the river water could favour adsorption and differential loss of certain CDOM components (Uher et al., 2001) well before the freshwater−saltwater transition.

Another loss process that could differentially affect CDOM across the MR estuary is photochemical degradation of DOM. This process is known to be important in CDOM-rich waters, including estuaries (Köhler et al., 2002). There is experimental and modeling evidence of UV-photodegradation in the Beaufort Sea region, however, the strong attenuation of UV radiation by particles and CDOM within these waters, and also by the sea ice that covers the region well into summer, means that this process likely consumes only a small fraction of total riverine DOM (Bélanger et al., in press).

Bacterial degradation processes are also likely to exert an influence on DOM characteristics. An analysis of prokaryotic community structure in the MR region, conducted in parallel to the present study, showed that both the river and the inshore environments contained high concentrations of Bacteria and also Archaea (Garneau et al., 2006; Galand et al., 2006). The former taxonomic domain contained representatives from several classes including the *Cytophaga−Flavobacterium* cluster, bacteria known to have wide substrate preferences (Kirchman, 2002). These results implied a high metabolic diversity and an ability to break down a broad range of organic substrates. However, the near zero seawater temperatures in the arctic coastal ocean maintain the catabolic activity of heterotrophic prokaryotes at slow rates (Garneau et al., 2006), and this process is unlikely to account for rapid changes in DOM concentration across the salinity gradient. Bacterial degradation therefore seems unlikely to be the primary cause of the SFS gradients observed here. Similarly, in a study of bacterial degradation in the Yenisei River, this mechanism could account for a loss of only 4.5% of the total DOM across the estuary (Köhler et al., 2003).

A major feature that differentiates the two river systems is the hydrodynamic regime, and this may play a role in the pattern of CDOM change. The Great Whale River produces a relatively small plume that is rapidly mixed into the surrounding waters of Hudson Bay. Previous calculations have shown that the freshwater residence time inside this plume during mid-summer (in July−August) is approximately 12 h (Goldstein and Jacobsen, 1988), and the strong coastal jet that flows northwards along the eastern coast of Hudson Bay (Wang et al., 1994) is likely to advect the diluted river water rapidly away from the area. The Mackenzie River system produces a vast plume with a much longer residence time. A MODIS image from near the time of sampling, 26 August 2002, showed that the plume had a visible extent of $1787~km^2$. For an average water depth of the surface mixed layer of 5 m, this gives an estimated volume of $8.93~km^3$. The annual average discharge of the Mackenzie River is approximately $9730~m^3\,s^{-1}$ (Droppo et al., 1998), which would give a residence time in the plume of 10 days. However, the residence time is likely to be much longer than this because of recirculation processes that occur over the shallow Mackenzie Shelf. From hydrographic observations on these processes, Carmack et al. (2004) estimate that the residence time over the total shelf is likely to be greater than 6 months.

The prolonged residence time of freshwater over the Mackenzie Shelf would provide increased opportunity for all loss processes, and for an increased input of autochthonous DOM from *in situ* phytoplankton and sea ice production. This feature of the MR shelf system also implies that the coastal waters are an integration of the past several months of freshwater input, and that offshore patterns are a reflection of this timescale rather than conservative mixing or short-term biogeochemical dynamics. Consistent with this conclusion, the inshore marine SFS spectra were much more similar to the river spectra observed during the spring period of high discharge (MR3) than at the time of transect sampling (MR1

and MR2), with the exception of the strong autochthonous peak in MR3 that is likely to be subject to more rapid bacterial degradation. The Mackenzie River had much higher concentrations of particulate organic matter during the spring period of maximum discharge, and its DOC was also more coloured at this time. Much of the terrigenous CDOM flux to the coastal ocean is therefore likely to be timed in spring-early summer, and recirculation processes would allow this signature to be retained for several months over the shelf. The difference in hydraulic residence times between the MR and GWR systems may be an important factor contributing to their strikingly different offshore CDOM patterns.

In conclusion, our observations underscore the strong influence of DOM-rich rivers on the arctic coastal shelf environment. SFS analysis proved to be a valuable guide to DOM composition and revealed major differences between the Mackenzie and Great Whale rivers that likely reflect differences in catchment age and soil activity. The two systems also differed in their degree of change in DOM properties across the freshwater−saltwater transition. The SFS analysis implies that this may result from differences in the hydrodynamic regime and freshwater residence times of the two shelf regions. It is not known at present which of the two systems is more representative of arctic rivers in general, or whether each arctic river has its own distinctive DOM composition and inshore behaviour. Our Mackenzie River data show evidence of differences in organic matter quality and concentration between the spring snowmelt period and the fall period of lower discharge. More detailed temporal records are needed to assess these seasonal differences, as well as interannual and long-term trends. As the Arctic continues to warm up, DOM export by rivers to the continental shelf environment is likely to change in magnitude and composition. The inter-system variability observed in this study implies that there are large regional variations in these export processes that will need to be considered for monitoring and predicting future change in arctic coastal waters.

References

ACIA, 2004. Impacts of a Warming Arctic − Arctic Climate Impact Assessment. Cambridge University Press, New York, p. 144.

Belzile, C., Vincent, W.F., Gibson, J.A.E., Van Hove, P., 2001. Bio-optical characteristics of the snow, ice, and water column of perennially ice-covered lake in the high Arctic. Canadian Journal of Fisheries and Aquatic Science 58, 2405−2418.

Bélanger, S., Xie, H., Krotkov, N., Larouche, P., Vincent, W.F., Babin, M. Photomineralization of terrigenous dissolved organic matter in arctic coastal waters from 1979 to 2003: interannual variability and implications of climate change. Global Biogeochemical Cycles 20, GB4005, in press. doi:10.1029/2006GB002708.

Benner, R., Benitez-Nelson, B., Kaiser, K., Amon, R.M., 2004. Export of young terrigenous dissolved organic carbon from rivers to the Arctic Ocean. Geophysical Research Letters 31, L05305.

Blough, N.V., Del Vecchio, R., 2002. Chromophoric DOM in the coastal environment. In: Hansell, D., Carlson, C.A. (Eds.), Biogeochemistry of Marine Dissolved Organic Matter. Academic Press, Amsterdam, pp. 509−546.

Carmack, E.C., Macdonald, R.W., Jasper, S., 2004. Phytoplankton productivity on the Canadian Shelf of the Beaufort Sea. Marine Ecology Progress Series 277, 37−50.

Cassasas, E., Marques, I., Tauler, R., 1995. Study of acid−base properties of fulvic acids using fluorescence spectrometry and multivariate curve resolution methods. Analytica Chimica Acta 310, 473−484.

Cauwet, G., Sidorov, I., 1996. The biogeochemistry of Lena River: organic carbon and nutrients distribution. Marine Chemistry 53, 211−227.

Chen, J., Leboeuf, E.J., Dai, S., Gu, B., 2003. Fluorescence spectroscopic studies of natural organic matter fractions. Chemosphere 50, 639−647.

Dittmar, T., 2004. Evidence for terrigenous dissolved organic nitrogen in the Arctic deep sea. Limnology and Oceanography 49, 148−156.

Droppo, I.G., Jeffries, D., Jaskot, C., Backus, S., 1998. The prevalence of freshwater flocculation in cold regions: a case study from the Mackenzie River Delta, Northwest Territories, Canada. Arctic 51, 155−164.

Finlay, J., Neff, J., Zimov, S., Davydova, A., Davydov, S., 2006. Snowmelt dominance of dissolved organic carbon in high-latitude watersheds: Implications for characterization and flux of river DOC. Geophysical Research Letters 33, L10401. doi:10.1029/2006GL025754.

Galand, P.E., Lovejoy, C., Vincent, W.F., 2006. Remarkably diverse and contrasting archaeal communities in a large arctic river and the coastal Arctic Ocean. Aquatic Microbial Ecology 44, 115−126.

Garneau, M.-E., Vincent, W.F., Alonso-Sáez, L., Gratton, Y., Lovejoy, C., 2006. Prokaryotic community structure and heterotrophic production in a river-influenced coastal arctic ecosystem. Aquatic Microbial Ecology 42, 27−40.

Goldstein, S.J., Jacobsen, S.B., 1988. REE in the Great Whale River estuary, northwest Québec. Earth and Planetary Science Letters 88, 241−252.

Goñi, M.A., Yunker, M.B., Macdonald, R.W., Eglinton, T.I., 2005. The supply and preservation of ancient and modern components of organic carbon in the Canadian Beaufort Shelf of the Arctic Ocean. Marine Chemistry 93, 53.

Guéguen, C., Guo, L., Tanaka, N., 2005. Distributions and characteristics of colored dissolved organic matter in the Western Arctic Ocean. Continental Shelf Research 25, 1195−1207.

Gulledge, J., Schimel, J.P., 2000. Controls on soil carbon dioxide and methane fluxes in a variety of taiga forest stands in interior Alaska. Ecosystems 3, 269−282.

Guo, L., Lehner, J.K., White, D.M., Garland, D.S., 2003. Heterogeneity of natural organic matter from the Chena River, Alaska. Water Research 37, 1015−1022.

Hudon, C., Morin, R., Bunch, J., Harland, R., 1996. Carbon and nutrient output from the Great Whale River (Hudson Bay) and a comparison with other rivers around Québec. Canadian Journal of Fisheries and Aquatic Science 53, 1513–1525.

Kalbitz, K., Geyer, S., Geyer, W., 2000. A comparative characterization of dissolved organic matter by means of original aqueous samples and isolated humic substances. Chemosphere 40, 1305–1312.

Kalbitz, K., Geyer, W., 2001. Humification indices of water-soluble fulvic acids derived from synchronous fluorescence spectra-effects of spectrometer type and concentration. Journal of Plant Nutrition and Soil Sciences 164, 259–265.

Kendall, C., Silva, S.R., Kelly, V.J., 2001. Carbon and nitrogen isotopic composition of particulate organic matter in four large river systems across the United States. Hydrological Processes 15, 1301–1346.

Kirchman, D.L., 2002. The ecology of Cytophaga–Flavobacteria in aquatic environments. FEMS Microbial Ecology 39, 91–100.

Köhler, S., Buffam, I., Jonsson, A., Bishop, K., 2002. Photochemical and microbial processing of stream and soil water dissolved organic matter in a boreal forested catchment in northern Sweden. Aquatic Sciences 64, 269–281.

Köhler, H., Meon, B., Gordeev, V.V., Spitzy, A., Amon, R.M., 2003. Dissolved organic matter (DOM) in the estuaries of Ob and Yenisei and the adjacent Kara Sea, Russia. Proceedings in Marine Sciences 6, 281–309.

Kowalczuk, P., Cooper, W.J., Whitehead, R., Durako, M.J., Sheldon, W.J., 2003. Characterization of CDOM in an organic-rich river and surrounding coastal ocean in the South Atlantic Bight. Aquatic Sciences 65, 384–401.

Lehmann, M.K., Davis, R.F., Huot, Y., Cullen, J.J., 2004. Spectrally weighted transparency in models of water-column photosynthesis and photoinhibition by ultraviolet radiation. Marine Ecology Progress Series 269, 101–110.

Lobbes, J.M., Fitznar, H.P., Kattner, G., 2000. Biogeochemical characteristics of dissolved and particulate organic matter in Russian rivers entering the Arctic Ocean. Geochimica et Cosmochimica Acta 64, 2973–2983.

McKnight, D.M., Boyer, E.W., Westerhoff, P.K., Doran, P.T., Kulbe, T., Anderson, D.T., 2001. Spectrofluorometric characterization of dissolved organic matter for indication of precursor organic material aromaticity. Limnology and Oceanography 46, 38–48.

Miano, T.M., Senesi, N., 1992. Synchronous excitation fluorescence spectroscopy applied to soil humic substances chemistry. The Science of the Total Environment 117/118, 41–51.

Millie, D.F., Schofield, O.M., Kirkpatrick, G.J., Johnsen, G.P., Tester, A., Vinyard, B.T., 1997. Detection of harmful algal blooms using photopigments and absorption signatures: a case study of the Florida red tide dinoflagellate, Gymnodinium breve. Limnology and Oceanography 42, 1240–1251.

Millot, R., Gaillardet, J.E., Dupré, B., Allegre, C.J., 2003. Northern latitude chemical weathering rates: clues from the Mackenzie River Basin, Canada. Geochimica et Cosmochimica Acta 67, 1305–1329.

Minagawa, M., Iseki, K., Macdonald, R.W., 1991. Carbon and nitrogen isotope composition of organic matters in the Arctic food webs. La Mer 29, 209–211.

Mobed, J.J., Hemmingsen, S.L., Autry, J.L., McGown, L.B., 1996. Fluorescence characterization of IHSS humic substances: total luminescence spectra with absorbance correction. Environmental Science and Technology 30, 3061–3065.

Montgomery, S., Lucotte, M., Cournoyer, L., 2000. The use of stable carbon isotopes to evaluate the importance of fine suspended particulate matter in the transfer of methylmercury to biota in boreal flooded environments. The Science of the Total Environment 261, 33–41.

Naidu, A.S., Cooper, L.W., Finney, B.P., Macdonald, R.W., Alexander, C., Semiletov, I.P., 2000. Organic carbon isotope ratios ($\delta^{13}C$) of Arctic Amerasian continental shelf sediments. International Journal of Earth Sciences 89, 522–532.

Opsahl, S., Benner, R., Amon, R.M., 1999. Major flux of terrigenous dissolved organic matter through the Arctic Ocean. Limnology and Oceanography 44, 2017–2023.

Patra, D., Mishra, A.K., 2002. Recent developments in multi-component synchronous fluorescence scan analysis. Trends in Analytical Chemistry 21, 787–798.

Peterson, B.J., McClelland, J.W., Curry, R., Holmes, R.M., Walsh, J.E., Aagaard, K., 2006. Trajectory shifts in the arctic and subarctic freshwater cycle. Science 313, 1061–1066.

Peuravuori, J., Koivikko, R., Phlaja, K., 2002. Characterization, differentiation and classification of aquatic humic matter separated with different sorbents: synchronous scanning fluorescence spectroscopy. Water Research 36, 4552–4562.

Pienitz, R., Vincent, W.F., 2000. Effect of climate change relative to ozone depletion on UV exposure in subarctic lakes. Nature 404, 484–487.

Pullin, M.J., Cabaniss, S.E., 1995. Rank analysis of the pH-dependent synchronous fluorescence spectra of six humic substances. Environmental Science and Technology 29, 1460–1467.

Rachold, V., Eicken, H., Gordeev, V.V., Grigoriev, H., Hubberten, H.W., Lisitzin, A.P., Shevchenko, V.P., Schirrmeister, L., 2004. Modern terrigenous organic carbon input to the Arctic Ocean. In: Stein, R., Macdonald, R.W. (Eds.), The Organic Carbon Cycle in the Arctic Ocean. Springer-Verlag, Berlin, pp. 33–55.

Sharp, J.H., Benner, R., Bennett, L., Carlson, C.A., Dow, R., Fitzwater, S.E., 1993. Re-evaluation of high temperature combustion and chemical oxidation measurements of dissolved organic carbon in seawater. Limnology and Oceanography 38, 1774–1782.

Spears, B.M., Lesack, L.F.W., 2006. Bacterioplankton production, abundance, and nutrient limitation among lakes of the Mackenzie Delta (western Canadian arctic). Canadian Journal of Fisheries and Aquatic Sciences 63, 845–857.

Stedmon, C.A., Markager, S., Kaas, H., 2000. Optical properties and signatures of chromophoric dissolved organic matter (CDOM) in Danish coastal waters. Estuarine, Coastal and Shelf Science 51, 267–278.

Stedmon, C.A., Markager, S., 2003. Behaviour of the optical properties of coloured dissolved organic matter under conservative mixing. Estuarine, Coastal and Shelf Science 57, 973–979.

Telang, S.A., Pocklington, R., Naidu, A.S., Romankevich, E.A., Gitelson, I.I., Gladyshev, M.I., 1991. Carbon and mineral transport in major North American, Russian Arctic, and Siberian rivers: the St-Lawrence, the Mackenzie, the Yukon, the Arctic Alaskan Rivers, the Arctic Basin rivers in the Soviet Union, and the Yenisei. In: Degens, E.T., Kempe, S., Richey, J.E. (Eds.), SCOPE 42 Biogeochemistry of Major World Rivers. John Wiley & Sons, London, pp. 75–104.

Thurman, E.M., 1985. Organic Geochemistry of Natural Waters. Kluwer Academic Publishers Group, Dordrecht, 497 pp.

Uher, G., Hughes, C., Henry, G., Upstill-Goddard, R.C., 2001. Non-conservative mixing behavior of colored dissolved organic matter in a humic-rich, turbid estuary. Geophysical Research Letters 28, 3309–3312.

Velapoldi, R.A., Mielenz, K.D., 1980. Standard Reference Materials: A Fluorescence Standard Reference Material, Quinine Sulfate Dihydrate. In: National Bureau of Standards (U.S.) Special Publication. 260-64. National Measurement Laboratory, U.S. Department of Commerce, Washington, DC, 139 pp.

Waelbroeck, C., Monfray, P., 1997. The impact of permafrost thawing on the carbon dynamics of tundra. Geophysical Research Letters 24, 229–232.

Wang, J., Mysaki, L.A., Ingram, G.R., 1994. A three-dimensional numerical simulation of Hudson Bay summer ocean circulation: topographic gyres, separations, and coastal jets. Journal of Physical Oceanography 24, 2496–2514.

Yamamuro, M., Kayanne, H., 1995. Rapid direct determination of organic carbon and nitrogen in carbonate-bearing sediment with a Yanaco MT-5 CHN analyser. Limnology and Oceanography 40, 1001–1005.

Yunker, M.B., Macdonald, R.W., Veltkamp, D.J., Cretney, W.J., 1995. Terrestrial and marine biomarkers in a seasonally ice-covered arctic estuary-integration of multivariate and biomarker approaches. Marine Chemistry 49, 1–50.